# Lipid interactions are important for the Tol-Pal complex in maintaining outer membrane lipid homeostasis

Nadege Zi-Lin Lim[1,2], Robin A Corey[3,4], Wei-Chuen Poh[1], Phillip J Stansfeld[5], and Shu-Sin Chng[1,6,*]

**Affiliations:**

[1]Department of Chemistry, National University of Singapore, Singapore 117543

[2]National University of Singapore Graduate School for Integrative Sciences and Engineering, Singapore 117456

[3]Department of Biochemistry, University of Oxford, Oxford OX1 3QU, United Kingdom

[4]Current address: School of Physiology, Pharmacology and Neuroscience, University of Bristol, Bristol BS8 1TD, United Kingdom

[5]School of Life Sciences and Department of Chemistry, University of Warwick, Coventry CV4 7AL, United Kingdom

[6]Singapore Center for Environmental Life Sciences Engineering, National University of Singapore (SCELSE-NUS), Singapore 117456

*To whom correspondence should be addressed

**E-mail:** chmchngs@nus.edu.sg

**Abstract:**

Gram-negative bacteria are intrinsically resistant to many antibiotics in part due to the asymmetric architecture and barrier function of their outer membrane (OM). To establish proper lipid asymmetry, cells need to ensure an intricate balance of constituent OM components, especially lipids. In this regard, the conserved, trans-envelope Tol-Pal complex plays a primary role in maintaining OM lipid homeostasis, thus OM integrity, possibly via retrograde phospholipid transport. However, mechanistic details for this process are unknown, owing to the lack of evidence for direct lipid binding. In this study, we discover that the periplasmic protein TolB, a key component of the Tol-Pal system, associates directly with membranes in vitro, via specific interactions with cardiolipin (CL). Using coarse-grained molecular dynamics simulations, we identify a CL-binding site on TolB; a single amino acid mutation at this site abolishes in vitro membrane interaction, consequently impairing cellular Tol-Pal function in maintaining OM homeostasis in *Escherichia coli*. Curiously, we find that the functional requirement for TolB-CL interactions can be partially bypassed in cells lacking CL, suggesting compensatory effects through other lipids only when CL is absent. Our findings reveal a previously unappreciated lipid-binding role for TolB, and provide novel insights into how the Tol-Pal complex may facilitate phospholipid transport across the cell envelope. Our work will inform future strategies towards developing new antibiotics against Gram-negative bacteria.

38 **Introduction:**

39 Gram-negative infections pose a significant threat to global health due to existing/intrinsic and
40 emerging/acquired resistance to antibiotics.[1] A large part of such antibiotic resistance stems
41 from the formidable barrier conferred by the complex cell envelope, particularly the outer
42 membrane (OM), which encapsulates the peptidoglycan layer and the inner membrane (IM).[2]
43 Consequently, a great many efforts have been focused on understanding Gram-negative OM
44 biogenesis and homeostasis, culminating in well-established mechanisms for the assembly of
45 major OM components, including β-barrel proteins,[3] lipoproteins,[4] and lipopolysaccharides
46 (LPS).[5] Even so, little is known about the bidirectional transport of bulk phospholipids (PLs),
47 the most basic building block of any bilayer, across the cell envelope.[6-8] In this regard, AsmA
48 superfamily proteins and the Tol-Pal complex have only recently been implicated in
49 anterograde (IM-to-OM) and retrograde (OM-to-IM) PL transport, respectively.[9-13]

50 The Tol-Pal complex is critically important for OM stability and lipid homeostasis.[10, 11] In the
51 absence of the Tol-Pal complex, cells accumulate excess PLs in the OM; such lipid imbalance
52 gives rise to OM instability and permeability defects, characterized by hypervesiculation, and
53 severe sensitivity to antibiotics and detergents.[14-17] In fact, *tol-pal* deletion cells exhibit slower
54 retrograde PL transport, suggesting critical involvement in the process.[11] The Tol-Pal complex
55 is also involved in cell division; constituent components are enriched at mid-cell during division,
56 and mutants display defects in OM constriction, and/or septal cell wall separation (under
57 hypoosmotic conditions).[18, 19] However, it has now been established that septal localization of
58 the Tol-Pal complex is not required for OM integrity, underscoring its primary role in OM lipid
59 homeostasis and transport.[10]

60 The Tol-Pal complex comprises the TolQRA and TolB-Pal sub-complexes at the IM and the
61 OM, respectively.[20] Pal is an OM lipoprotein that either binds the cell wall,[21-23] thus tethering
62 the OM, or interacts with the periplasmic protein TolB.[21, 24] The TolQRA sub-complex
63 harnesses the proton motive force (pmf) to transduce a force on the TolB-Pal sub-complex,
64 through TolA-TolB interaction across the cell envelope.[20] While such force transduction is
65 believed to be important for localization of Pal to the division site, and is hijacked by colicins
66 for cellular entry,[20] how the same mechanism contributes to the main function of the Tol-Pal
67 complex in OM lipid homeostasis is unclear.[10, 11, 18, 25] It has been proposed that the Tol-Pal
68 complex directly mediates retrograde transport of bulk PLs.[11] Yet, there is no evidence of lipid
69 binding by any of the Tol-Pal components.

70 In this study, we establish that the function of TolB requires direct interaction with membranes,
71 with specificity for a particular PL species, cardiolipin (CL). While trying to characterize TolB-

Pal interaction at the membrane in vitro, we serendipitously discover that TolB alone binds directly to liposomes. In addition, we find that this membrane association depends on the presence of CL, both in vitro and in silico. Furthermore, molecular dynamics (MD) simulations revealed a putative CL-binding site on TolB; we demonstrate that a specific mutation at this site disrupts TolB interactions with CL-containing membranes, as well as its cellular function. Our work underscores the functional relevance of TolB-membrane association, and provides novel insights into how the Tol-Pal complex may mediate PL transport.

## Results:

### TolB interacts with membranes

We initially set out to study how TolB interacts with Pal in a native environment. The strong interaction between TolB and Pal was previously observed using purified full-length TolB and truncated Pal proteins that are entirely soluble in aqueous solution.[24] However, full-length Pal is a lipoprotein anchored to the inner leaflet of the OM via its N-terminal triacyl modification, and it is not known how the TolB-Pal interaction may be affected at/near a lipid bilayer. Therefore, we reconstituted Pal into liposomes, and examine its interaction with TolB using isothermal calorimetry (ITC). In our proteoliposomes derived from *E. coli* polar lipids, ~80% of Pal is anchored on the surface, accessible to TolB added in the external solution (Fig S1). We first showed that control titrations of TolB into buffer or buffer into Pal proteoliposomes gave negligible background heat changes. Interestingly, we also did not observe significant signals between TolB and Pal proteoliposomes, in contrast to strong heat changes detected between TolB and soluble Pal under identical conditions (Fig 1A).[24] This unexpected result suggests either that TolB cannot bind Pal at the membrane, or that other interactions, possibly with the bilayer, mask TolB-Pal binding.

We hypothesized that TolB may interact with membranes, therefore titrated TolB into empty liposomes made from *E. coli* polar lipids, comprising phosphatidylethanolamine (PE): phosphatidylglycerol (PG):CL in a ratio of ~67:23:10. Remarkably, we detected endothermic heat changes between TolB and liposomes. As a control, the soluble domain of the OM lipoprotein LolB (sLolB) exhibited no interaction with empty liposomes (Fig 1B).[4] Furthermore, we found that TolB, but not sLolB, affected the sedimentation of liposomes in an in vitro assay (Fig S2). Taken together, our results demonstrate that TolB interacts directly with the lipid bilayer.

105 **TolB exhibits specificity for CL binding**

106 To understand the nature of interaction between TolB and the lipid bilayer, we also examined
107 TolB binding to empty liposomes derived from synthetic lipids representing major species in *E.*
108 *coli* (PE:PG 3:1). Interestingly, we did not observe any heat changes when TolB was titrated
109 into these synthetic lipid liposomes (Fig 1B). TolB also did not impact these liposomes during
110 sedimentation in vitro (Fig S2), consistent with the lack of interaction. A notable distinction
111 between liposomes derived from synthetic lipids or *E. coli* polar lipids is the presence of CL in
112 the latter, suggesting that TolB interacts with membranes in a CL-dependent manner.

113 To explore the possibility of TolB-CL interaction, we conducted interaction studies in silico
114 using coarse-grained (CG) molecular dynamics (MD) simulations. We positioned TolB ~8 nm
115 from membranes approximating our in vitro setup, namely PE:PG:CL at 67:23:10 (+CL), or
116 PE:PG at 75:25 (-CL). By running 5 x 10 μs simulations in each condition, we were able to
117 follow prospective interactions of TolB with either membrane. In the absence of CL, the
118 distance between TolB and the bilayer fluctuated constantly, indicating brief and unstable
119 interactions (Fig 2A). In stark contrast, when CL is present, TolB rapidly binds to the bilayer
120 and stays bound throughout the simulations (Fig 2A). Averaging the overall time that TolB
121 remains bound to the membrane (in all binding poses) over the 5 runs revealed an extremely
122 high membrane binding likelihood in the presence of CL, ca. 91% vs 39% when CL was absent.
123 These data corroborate our experimental observation that TolB interacts with membranes in a
124 CL-dependent manner.

125

126 **Disrupting the CL binding ability of TolB abolishes its function in OM lipid homeostasis**

127 We employed PyLipID, a software tool designed for predicting lipid binding sites within proteins,
128 to identify possible CL binding sites on TolB based on our CG-MD data.[26, 27] PyLipID enables
129 the calculation of residence times and binding probabilities between proteins and lipid
130 molecules from MD simulations. Our analysis revealed that TolB indeed harbors a CL-binding
131 site, which remained occupied with CL for ~81% of the total simulation time, clustering on
132 average ~4.4 CL molecules via their head groups (Fig 2B). Considering binding through this
133 site alone, membrane binding likelihood of TolB effectively reduced to zero in the absence of
134 CL (Fig 2C). TolB contains a C-terminal six-bladed β-propeller domain linked to a short peptide,
135 termed the 'TolA box', at the N terminus, via a α/β globular domain.[28] The TolA box and the β-
136 propeller domain interact with TolA and Pal, respectively.[24, 28, 29] The putative CL-binding site
137 comprises residues from 4 adjacent loop regions in the β-propeller domain of TolB, collectively
138 presenting 4 positively charged side chains ($Arg^{223}$, $Arg^{244}$, $Lys^{264}$, $Arg^{287}$) for interaction with

139 the phosphate moieties in the CL head groups (Fig 2D).[27] These Arg/Lys residues, along with
140 neighbouring side chains, all exhibit ~60% median CL occupancy (Fig 2B).

141 To investigate the importance of the putative CL-binding site, we substituted each Arg/Lys
142 position with either alanine or glutamate, and assessed whether these mutations perturbed
143 TolB function. The alanine variants behaved similarly to wild-type TolB (Fig 3A). Remarkably,
144 we found that R244E rendered this TolB charge-swapped variant incapable of rescuing
145 sensitivity to SDS-EDTA and vancomycin in the Δ*tolB* strain (Fig 3A, 4A), as well as the
146 increased cell width phenotype associated with OM lipid dyshomeostasis (Fig 4B).[10]
147 Importantly, this mutation did not impact TolB stability (Fig S3A), its ability to facilitate colicin A
148 entry (Fig S3B), nor its cellular interaction with Pal (Fig S4), indicating a true and specific loss
149 of function in maintaining OM integrity. In fact, we demonstrated that $TolB^{R244E}$ failed to restore
150 OM defects in a strain expressing a chimeric version of the Tol-Pal complex, whose only
151 function is in OM lipid homeostasis along the cell periphery (Fig 3B).[10] These findings indicate
152 that the functional impairment caused by the R244E mutation is most likely directly linked to
153 the disruption of TolB-CL binding.

154 R244 occupies a central position within the predicted CL-binding site. Therefore, we
155 hypothesize that changing this positively charged residue to a negative one (R244E) could
156 introduce repulsive interactions with the negatively charged head groups of CL, and disrupt
157 binding. Consistent with this idea, introduction of R244E in silico significantly reduced the
158 binding likelihood of TolB to CL-containing membranes, to ~49% chance (Fig 3C). We further
159 demonstrated that $TolB^{R244E}$ no longer exhibits significant heat changes when titrated into
160 liposomes derived from *E. coli* polar lipids (Fig 3D), indicating loss of its ability to bind CL.
161 $TolB^{R244E}$ also does not affect liposome sedimentation (Fig S5). Taken together, we conclude
162 that CL binding via R244 is critical for TolB function as part of the Tol-Pal complex to maintain
163 OM lipid homeostasis in wild-type cells.

164

165 **The requirement for TolB-CL binding for OM lipid homeostasis is partially bypassed in**
166 **strains lacking CL**

167 Since CL binding is important for TolB function, one might expect CL-deficient strains to exhibit
168 phenotypes associated with an impaired Tol-Pal complex. However, we found that Δ*clsABC*
169 mutations (Δ*cls*) do not cause apparent OM permeability defects (Fig S6). These observations
170 suggest that the presence of CL may not be strictly essential for Tol-Pal function in these cells.
171 To further test this idea, we examined whether the CL binding ability of TolB is still required in
172 the Δ*cls* mutant. $TolB^{R244E}$ was produced at comparable levels to wild-type TolB in Δ*tolB* strains
173 (Fig S7). To our surprise, $TolB^{R244E}$ was able to partially rescue sensitivity of Δ*cls* Δ*tolB* strain

174 to SDS-EDTA and vancomycin (Fig 4A). This mutation was even able to rescue the width
175 defect in Δ*tolB* cells in the absence of CL (Fig 4B), overall demonstrating that TolB$^{R244E}$ remains
176 functional in OM lipid homeostasis in cells lacking CL. Collectively, our results suggest that
177 although CL binding is important for TolB activity in wild-type cells, this requirement is partially
178 bypassed when CL is absent, potentially due to compensatory changes in the membrane
179 environment.

180

181 **TolB-CL binding is important for proper cell division**

182 Despite having a primary function in maintaining OM lipid homeostasis, the Tol-Pal complex
183 is recruited to mid-cell to facilitate OM invagination and/or septal cell wall separation. These
184 roles during cell division are thought to involve Pal-mediated OM-cell wall tethering,
185 modulation of cell wall enzymes, and/or possible OM lipid remodelling.[10, 18, 19] We examined
186 the impact of TolB$^{R244E}$ on cell division phenotypes, and found that wild-type cells expressing
187 this variant alone exhibited impaired growth and cell chaining under low osmolarity conditions
188 (Fig S8). Interestingly, expressing TolB$^{R244E}$ partially rescued growth defects, though not cell
189 chaining in the Δ*cls* mutant. Using TolB-sfGFP constructs expressed at comparable levels (Fig
190 S9), we showed that R244E did not affect enrichment of TolB to the mid cell in either wild-type
191 or Δ*cls* strains, under normal osmolarity conditions (Fig 5A and B). Furthermore, Pal-mCherry
192 still localized to the cell septum in the presence of TolB$^{R244E}$ regardless of whether CL was
193 available, albeit less strongly than in strains expressing wild-type TolB (Fig 5C and D).
194 Therefore, Pal-mediated OM-cell wall tethering at the division site is still significant when
195 TolB$^{R244E}$ is present, as opposed to no tethering in the absence of TolB. We conclude that loss
196 of TolB-CL binding may impact cell division instead via its effect on OM lipid homeostasis.

197

198 **<u>Discussion:</u>**

199 How the Tol-Pal complex maintains OM lipid homeostasis has remained elusive. While it has
200 been implicated in retrograde transport of bulk PLs, there has been a lack of evidence for any
201 protein-lipid interaction within the Tol-Pal complex.[10, 11] In this study, we have uncovered the
202 ability of the periplasmic protein, TolB, to bind lipid membranes in a CL-specific manner. We
203 have shown that disruption of a putative CL-binding site on TolB abolished binding of CL-
204 containing membranes, and impaired overall cellular function in OM lipid homeostasis.
205 Interestingly, CL-binding became somewhat dispensable for Tol-Pal function in cells lacking
206 CL, suggesting possible compensatory effects of other membrane lipids only when CL is

207 absent. Overall, our work provides critical insights into the direct involvement of the Tol-Pal
208 complex in lipid transport.

209 The discovery of TolB-CL interaction facilitates new ideas on how the Tol-Pal complex may
210 maintain OM lipid homeostasis and transport. Due to its cone-shaped structure, CL is generally
211 believed to be a non-bilayer lipid, which may preferentially localize to membrane regions of
212 high (negative) curvature.[30] This property is often attributed for why CL is enriched at the cell
213 poles,[31] albeit along with PG, a cylindrical bilayer lipid. In this vein, it is possible that CL would
214 be found in other highly curved or strained membrane regions around the cell periphery. In
215 cells lacking the Tol-Pal complex, excess PLs accumulate in the OM,[11] which may induce local
216 "ruffling" of the membrane, particularly in the inner leaflet. We speculate that CL may localize
217 to such bulges in the OM, presumably of high curvature, therefore marking sites of excess
218 lipids for TolB recognition. This process could be aided by Pal binding to TolB, positioning TolB
219 closer to the inner leaflet of the OM. Binding of TolB to CL at these sites may facilitate
220 subsequent interactions with TolA, which exerts a pulling force via the TolQR motor-stator
221 complex at the IM. Therefore, CL may serve as a spatial cue for TolB recruitment, enabling
222 the Tol-Pal complex to possibly mediate lipid transport, and maintain OM homeostasis. It is
223 likely that CL is the dominant non-bilayer lipid that accumulates at sites of high curvature,
224 explaining the requirement for TolB-CL binding in wild-type cells. In the absence of CL, and
225 only so, we reason that other non-bilayer lipids, e.g. PA or PE, could then play compensatory
226 role(s), rendering TolB-CL interactions non-essential. Further (biophysical) characterization of
227 TolB-membrane binding will be critical. Given the essential role of TolB in OM homeostasis, its
228 membrane-binding activity could be exploited as a potential drug target.

229 The primary function of the Tol-Pal complex is to maintain OM lipid homeostasis, possibly via
230 retrograde PL transport.[10, 11] In this context, given its ability to bind membranes via CL (head
231 groups), TolB is quite likely the main effector. However, it is unlikely that TolB moves CL as a
232 specific cargo, since cells lacking the Tol-Pal complex accumulate excess major PLs, not only
233 CL, in the OM.[11] Interestingly, the identified binding site to CL lies in the C-terminal β-propeller
234 domain of TolB, lining the region(s) where TolB interacts with colicins or with Pal.[24, 32] Instead,
235 we propose that TolB binding to CL at membrane bulges may allow its N-terminal "TolA box"
236 to become accessible (to TolA), similar to the effect of binding to colicins. The pulling force
237 thus transduced by the TolQRA complex on TolB and its associated OM leaflet could bring this
238 assembly closer to the IM, eventually leading to hemifusion, and possibly retrograde diffusion
239 of PLs across a membrane bridge.[13] Here, the role of Pal as a cell wall anchor may define
240 permissive sites across the peptidoglycan mesh, and facilitate such trans-envelope membrane
241 dynamics while preserving overall cell envelope integrity. This mechanistic working model,

242 while speculative, provides a useful framework for our continued understanding of the Tol-Pal
243 complex and its function in OM lipid homeostasis and transport in Gram-negative bacteria.

## Material and Methods:

### Strains, plasmids, and growth conditions

The strains, plasmids and primers used were summarized in Table S1-4. All strains were grown in lysogeny broth (LB – 1% (w/v) tryptone and 0.5% (w/v) yeast extract with or without 1% (w/v) NaCl) liquid culture at 37 ºC or on solid LB agar plates (1.5% (w/v) Bacto-Agar added to LB media) supplemented with ampicillin (100 µg/mL), spectinomycin (20 µg/mL), chloramphenicol (30 µg/mL), 1 mM Isopropyl β-D-1-thiogalactopyranoside (IPTG). The gene deletion alleles were constructed using λ Red recombination and transduced into strains using P1 transduction.[33] Plasmids expressing TolB-sfGFP, Pal-mCherry, TolB-Pal-mCherry were constructed using Gibson assembly.[34]

### Isothermal Calorimetry (ITC)

TolB, sPal and Pal proteoliposomes in PBS were used for ITC. All proteins used in the experiment were in the same buffer (20 mM phosphate, 300 mM NaCl) to ensure no heat release from the mixture of different buffers. Prior to performing ITC, samples were centrifuged (10,000 x *g*, 4 ºC, 5mins) to remove any precipitate. ITC was carried using NanoITC Microcalorimeter (TA Instruments). 50 µL of TolB at concentration of 140 µM (7 nmol) was injected into 20µM (166 µL, 3.32 nmol) of sPal or Pal proteoliposomes over 48 injections with an interval of 220 seconds. Experiments were carried out at 25 ºC. 4.15 nmol of Pal proteins were used to generate Pal proteoliposomes, with ~80% surface-exposed (~3.32 nmol).

### Coarse-grained molecular dynamics simulations

Membrane binding of TolB was assayed using coarse-grained (CG) simulations. The monomeric TolB crystal structure was used as an input [Protein Data Bank ID code 2W8B; chain A.[24] Protein atoms were converted to the CG Martini 3 force field[35] using the martinize2 method.[36] Additional bonds of 500 kJ mol$^{-1}$ nm$^{-2}$ were applied between all protein backbone beads within 1 nm. Proteins were oriented randomly using the Gromacs *editconf* tool, with a different starting orientation for each repeat. Proteins were placed 8 nm from a membrane (centre-of-mass distance), which were built using the insane protocol.[37] Simulation boxes were 11 x 11 x 21 nm. All systems were solvated with Martini waters and $Na^+$ and $Cl^-$ ions to a neutral charge and 150 mM. Systems were minimized using the steepest descents method, followed by 1 ns equilibration with 5 fs time steps, then by 100 ns equilibration with 20 fs time steps, before 10 x 10 µs production simulations using 20 fs time steps, all in the NPT ensemble at 323 K with the V-rescale thermostat ($\tau_t$ = 1.0 ps) and semi-isotropic Parrinello-Rahman pressure coupling at 1 bar ($\tau_p$ = 12.0 ps). The Reaction-Field method was used to model long-range electrostatic interactions. Bond lengths were constrained to their equilibrium values

278 using the LINCS algorithm. Simulations were run in Gromacs 2020.3.[38, 39] Plots were made
279 using Prism 10. MD snapshots were made using VMD.[40] Data were analysed using Gromacs
280 tools and the PyLipID package.[26]

281 **Efficiency of plating (EOP)**

282 Strains were grown to mid-log ($OD_{600}$ ~0.6) and normalized to an $OD_{600}$ of 0.1. 10-fold dilution
283 was performed to obtain a range of concentration of strains. 5µL of these diluted cultures were
284 spotted on LB agar plates containing 0.5% sodium dodecyl sulfate (SDS)/ 0.5 mM
285 Ethylenediaminetetraacetic acid (EDTA), 60 µg/mL vancomycin or without NaCl, unless
286 otherwise stated. The LB agar plates were then incubated at 37 °C (for SDS EDTA and
287 vancomycin plates) or at 42 °C (for plates without NaCl) for approximately 18hrs. All results
288 shown are representative of at least three independent replicates.

289 **Microscopy**

290 Overnight cultures of the strains were grown in LB and diluted (1:2000) in fresh media. The
291 sub-cultures were grown to mid-log (~ 3 hrs) and concentrated 10-fold by centrifugation (3,000
292 x *g*, 5 mins). 10 µL of the sample was spotted on an agarose pad (1% agarose, in LB medium)
293 and viewed under a confocal microscope (Olympus FV3000 Confocal Microscope). Images
294 were analysed using ImageJ/FIJI (version 1.53c) and the MicrobeJ (version 5.13I) plugin.[41, 42]

295

296 **Acknowledgements:**

297 The authors would like to thank Jiang Hui Wu for her initial contributions in identifying residues
298 for TolB-Pal crosslinking. We are grateful to Denis Duché (CNRS, Aix-Marseille Université) for
299 providing the α-TolB and α-Pal antisera. We also thank Wee Boon Tan for useful and critical
300 discussions. N.Z.-L.L. was supported by the National University of Singapore Graduate
301 School of Integrative Sciences and Engineering Scholarship (ISEP). This work was supported
302 by the Singapore Ministry of Health National Medical Research Council under its Open Fund
303 Individual Research Grant (MOH-000145) and the Singapore Ministry of Education Academic
304 Research Fund Tier 1 grant (National University of Singapore-Faculty of Science Preparatory
305 Grant Scheme) (both to S.-S.C.). R.A.C. was funded by Wellcome (208361/Z/17/Z). P.J.S.'s
306 lab was funded by Wellcome, MRC, BBSRC, EPSRC, NIH, JPIAMR and the Howard Dalton
307 Centre. This project made use of time on ARCHER2 granted via the UK High-End Computing
308 Consortium for Biomolecular Simulation, HECBioSim (http://www.hecbiosim.ac.uk), supported
309 by EPSRC (grant no. EP/R029407/1). P.J.S. would like to thank the SCRTP at Warwick for
310 use of the computing infrastructure. P.J.S. acknowledges Sulis at HPC Midlands+, which was
311 funded by the EPSRC on grant EP/T022108/1.

The authors declare that they have no conflict of interest.

## References:


1. Organization, W. H., *WHO bacterial priority pathogens list, 2024: bacterial pathogens of public health importance, to guide research, development, and strategies to prevent and control antimicrobial resistance*. World Health Organization: 2024.
2. Nikaido, H., Molecular basis of bacterial outer membrane permeability revisited. *Microbiol Mol Biol Rev* **2003,** *67* (4), 593-656.
3. Tomasek, D.; Kahne, D., The assembly of β-barrel outer membrane proteins. *Curr Opin Microbiol* **2021,** *60*, 16-23.
4. Okuda, S.; Tokuda, H., Lipoprotein Sorting in Bacteria. *Annual Review of Microbiology* **2011,** *65* (Volume 65, 2011), 239-259.
5. Simpson, B. W.; May, J. M.; Sherman, D. J.; Kahne, D.; Ruiz, N., Lipopolysaccharide transport to the cell surface: biosynthesis and extraction from the inner membrane. *Philosophical Transactions of the Royal Society B: Biological Sciences* **2015,** *370* (1679), 20150029.
6. Jones, N. C.; Osborn, M. J., Translocation of phospholipids between the outer and inner membranes of Salmonella typhimurium. *J Biol Chem* **1977,** *252* (20), 7405-12.
7. Donohue-Rolfe, A. M.; Schaechter, M., Translocation of phospholipids from the inner to the outer membrane of Escherichia coli. *Proc Natl Acad Sci U S A* **1980,** *77* (4), 1867-71.
8. Langley, K. E.; Hawrot, E.; Kennedy, E. P., Membrane assembly: movement of phosphatidylserine between the cytoplasmic and outer membranes of Escherichia coli. *J Bacteriol* **1982,** *152* (3), 1033-41.
9. Ruiz, N.; Davis, R. M.; Kumar, S., YhdP, TamB, and YdbH Are Redundant but Essential for Growth and Lipid Homeostasis of the Gram-Negative Outer Membrane. *mBio* **2021,** *12* (6), e0271421.
10. Tan, W. B.; Chng, S.-S., Primary role of the Tol-Pal complex in bacterial outer membrane lipid homeostasis. *Nature Communications* **2025,** *16* (1), 2293.
11. Shrivastava, R.; Jiang, X. E.; Chng, S.-S., Outer membrane lipid homeostasis via retrograde phospholipid transport in Escherichia coli. *Molecular Microbiology* **2017,** *106* (3), 395-408.
12. Douglass, M. V.; McLean, A. B.; Trent, M. S., Absence of YhdP, TamB, and YdbH leads to defects in glycerophospholipid transport and cell morphology in Gram-negative bacteria. *PLoS Genet* **2022,** *18* (2), e1010096.
13. Tan, W. B.; Chng, S. S., How Bacteria Establish and Maintain Outer Membrane Lipid Asymmetry. *Annu Rev Microbiol* **2024,** *78* (1), 553-573.
14. Bernadac, A.; Gavioli, M.; Lazzaroni, J. C.; Raina, S.; Lloubès, R., Escherichia coli tol-pal mutants form outer membrane vesicles. *J Bacteriol* **1998,** *180* (18), 4872-8.
15. Lloubès, R.; Cascales, E.; Walburger, A.; Bouveret, E.; Lazdunski, C.; Bernadac, A.; Journet, L., The Tol-Pal proteins of the Escherichia coli cell envelope: an energized system required for outer membrane integrity? *Res Microbiol* **2001,** *152* (6), 523-9.
16. Lopes, J.; Gottfried, S.; Rothfield, L., Leakage of periplasmic enzymes by mutants of Escherichia coli and Salmonella typhimurium: isolation of "periplasmic leaky" mutants. *J Bacteriol* **1972,** *109* (2), 520-5.
17. Kowata, H.; Tochigi, S.; Kusano, T.; Kojima, S., Quantitative measurement of the outer membrane permeability in Escherichia coli lpp and tol–pal mutants defines the significance of Tol–Pal function for maintaining drug resistance. *The Journal of Antibiotics* **2016,** *69* (12), 863-870.

18. Gerding, M. A.; Ogata, Y.; Pecora, N. D.; Niki, H.; de Boer, P. A., The trans-envelope Tol-Pal complex is part of the cell division machinery and required for proper outer-membrane invagination during cell constriction in E. coli. *Mol Microbiol* **2007,** *63* (4), 1008-25.
19. Yakhnina, A. A.; Bernhardt, T. G., The Tol-Pal system is required for peptidoglycan-cleaving enzymes to complete bacterial cell division. *Proceedings of the National Academy of Sciences* **2020,** *117* (12), 6777-6783.
20. Szczepaniak, J.; Press, C.; Kleanthous, C., The multifarious roles of Tol-Pal in Gram-negative bacteria. *FEMS Microbiol Rev* **2020,** *44* (4), 490-506.
21. Bouveret, E.; Bénédetti, H.; Rigal, A.; Loret, E.; Lazdunski, C., In vitro characterization of peptidoglycan-associated lipoprotein (PAL)-peptidoglycan and PAL-TolB interactions. *J Bacteriol* **1999,** *181* (20), 6306-11.
22. Lazzaroni, J. C.; Portalier, R., The excC gene of Escherichia coli K-12 required for cell envelope integrity encodes the peptidoglycan-associated lipoprotein (PAL). *Mol Microbiol* **1992,** *6* (6), 735-42.
23. Parsons, L. M.; Lin, F.; Orban, J., Peptidoglycan recognition by Pal, an outer membrane lipoprotein. *Biochemistry* **2006,** *45* (7), 2122-8.
24. Bonsor, D. A.; Hecht, O.; Vankemmelbeke, M.; Sharma, A.; Krachler, A. M.; Housden, N. G.; Lilly, K. J.; James, R.; Moore, G. R.; Kleanthous, C., Allosteric β-propeller signalling in TolB and its manipulation by translocating colicins. *The EMBO Journal* **2009,** *28* (18), 2846-2857-2857.
25. Nagel de Zwaig, R.; Luria, S. E., Genetics and physiology of colicin-tolerant mutants of Escherichia coli. *J Bacteriol* **1967,** *94* (4), 1112-23.
26. Song, W.; Corey, R. A.; Ansell, T. B.; Cassidy, C. K.; Horrell, M. R.; Duncan, A. L.; Stansfeld, P. J.; Sansom, M. S. P., PyLipID: A Python Package for Analysis of Protein–Lipid Interactions from Molecular Dynamics Simulations. *Journal of Chemical Theory and Computation* **2022,** *18* (2), 1188-1201.
27. Corey, R. A.; Song, W.; Duncan, A. L.; Ansell, T. B.; Sansom, M. S. P.; Stansfeld, P. J., Identification and assessment of cardiolipin interactions with E. coli inner membrane proteins. *Sci Adv* **2021,** *7* (34).
28. Abergel, C.; Bouveret, E.; Claverie, J. M.; Brown, K.; Rigal, A.; Lazdunski, C.; Bénédetti, H., Structure of the Escherichia coli TolB protein determined by MAD methods at 1.95 A resolution. *Structure* **1999,** *7* (10), 1291-300.
29. Szczepaniak, J.; Holmes, P.; Rajasekar, K.; Kaminska, R.; Samsudin, F.; Inns, P. G.; Rassam, P.; Khalid, S.; Murray, S. M.; Redfield, C.; Kleanthous, C., The lipoprotein Pal stabilises the bacterial outer membrane during constriction by a mobilisation-and-capture mechanism. *Nature Communications* **2020,** *11* (1), 1305.
30. Beltrán-Heredia, E.; Tsai, F.-C.; Salinas-Almaguer, S.; Cao, F. J.; Bassereau, P.; Monroy, F., Membrane curvature induces cardiolipin sorting. *Communications Biology* **2019,** *2* (1), 225.
31. Oliver, P. M.; Crooks, J. A.; Leidl, M.; Yoon, E. J.; Saghatelian, A.; Weibel, D. B., Localization of anionic phospholipids in Escherichia coli cells. *J Bacteriol* **2014,** *196* (19), 3386-98.
32. Zhang, Y.; Li, C.; Vankemmelbeke, M. N.; Bardelang, P.; Paoli, M.; Penfold, C. N.; James, R., The crystal structure of the TolB box of colicin A in complex with TolB reveals important differences in the recruitment of the common TolB translocation portal used by group A colicins. *Mol Microbiol* **2010,** *75* (3), 623-36.
33. Datsenko, K. A.; Wanner, B. L., One-step inactivation of chromosomal genes in Escherichia coli K-12 using PCR products. *Proceedings of the National Academy of Sciences* **2000,** *97* (12), 6640-6645.

34. Gibson, D. G.; Young, L.; Chuang, R.-Y.; Venter, J. C.; Hutchison, C. A.; Smith, H. O., Enzymatic assembly of DNA molecules up to several hundred kilobases. *Nature Methods* **2009,** *6* (5), 343-345.
35. Souza, P. C. T.; Alessandri, R.; Barnoud, J.; Thallmair, S.; Faustino, I.; Grünewald, F.; Patmanidis, I.; Abdizadeh, H.; Bruininks, B. M. H.; Wassenaar, T. A.; Kroon, P. C.; Melcr, J.; Nieto, V.; Corradi, V.; Khan, H. M.; Domański, J.; Javanainen, M.; Martinez-Seara, H.; Reuter, N.; Best, R. B.; Vattulainen, I.; Monticelli, L.; Periole, X.; Tieleman, D. P.; de Vries, A. H.; Marrink, S. J., Martini 3: a general purpose force field for coarse-grained molecular dynamics. *Nature Methods* **2021,** *18* (4), 382-388.
36. Kroon, P. C.; Grunewald, F.; Barnoud, J.; van Tilburg, M.; Souza, P. C. T.; Wassenaar, T. A.; Marrink, S. J., Martinize2 and Vermouth: Unified Framework for Topology Generation. eLife Sciences Publications, Ltd: 2024.
37. Wassenaar, T. A.; Ingólfsson, H. I.; Böckmann, R. A.; Tieleman, D. P.; Marrink, S. J., Computational Lipidomics with insane: A Versatile Tool for Generating Custom Membranes for Molecular Simulations. *Journal of Chemical Theory and Computation* **2015,** *11* (5), 2144-2155.
38. Abraham, M. J.; Murtola, T.; Schulz, R.; Páll, S.; Smith, J. C.; Hess, B.; Lindahl, E., GROMACS: High performance molecular simulations through multi-level parallelism from laptops to supercomputers. *SoftwareX* **2015,** *1-2*, 19-25.
39. Berendsen, H. J. C.; van der Spoel, D.; van Drunen, R., GROMACS: A message-passing parallel molecular dynamics implementation. *Computer Physics Communications* **1995,** *91* (1), 43-56.
40. Humphrey, W.; Dalke, A.; Schulten, K., VMD: Visual molecular dynamics. *Journal of Molecular Graphics* **1996,** *14* (1), 33-38.
41. Schindelin, J.; Arganda-Carreras, I.; Frise, E.; Kaynig, V.; Longair, M.; Pietzsch, T.; Preibisch, S.; Rueden, C.; Saalfeld, S.; Schmid, B.; Tinevez, J.-Y.; White, D. J.; Hartenstein, V.; Eliceiri, K.; Tomancak, P.; Cardona, A., Fiji: an open-source platform for biological-image analysis. *Nature Methods* **2012,** *9* (7), 676-682.
42. Ducret, A.; Quardokus, E. M.; Brun, Y. V., MicrobeJ, a tool for high throughput bacterial cell detection and quantitative analysis. *Nature Microbiology* **2016,** *1* (7), 16077.

436 **Figures:**

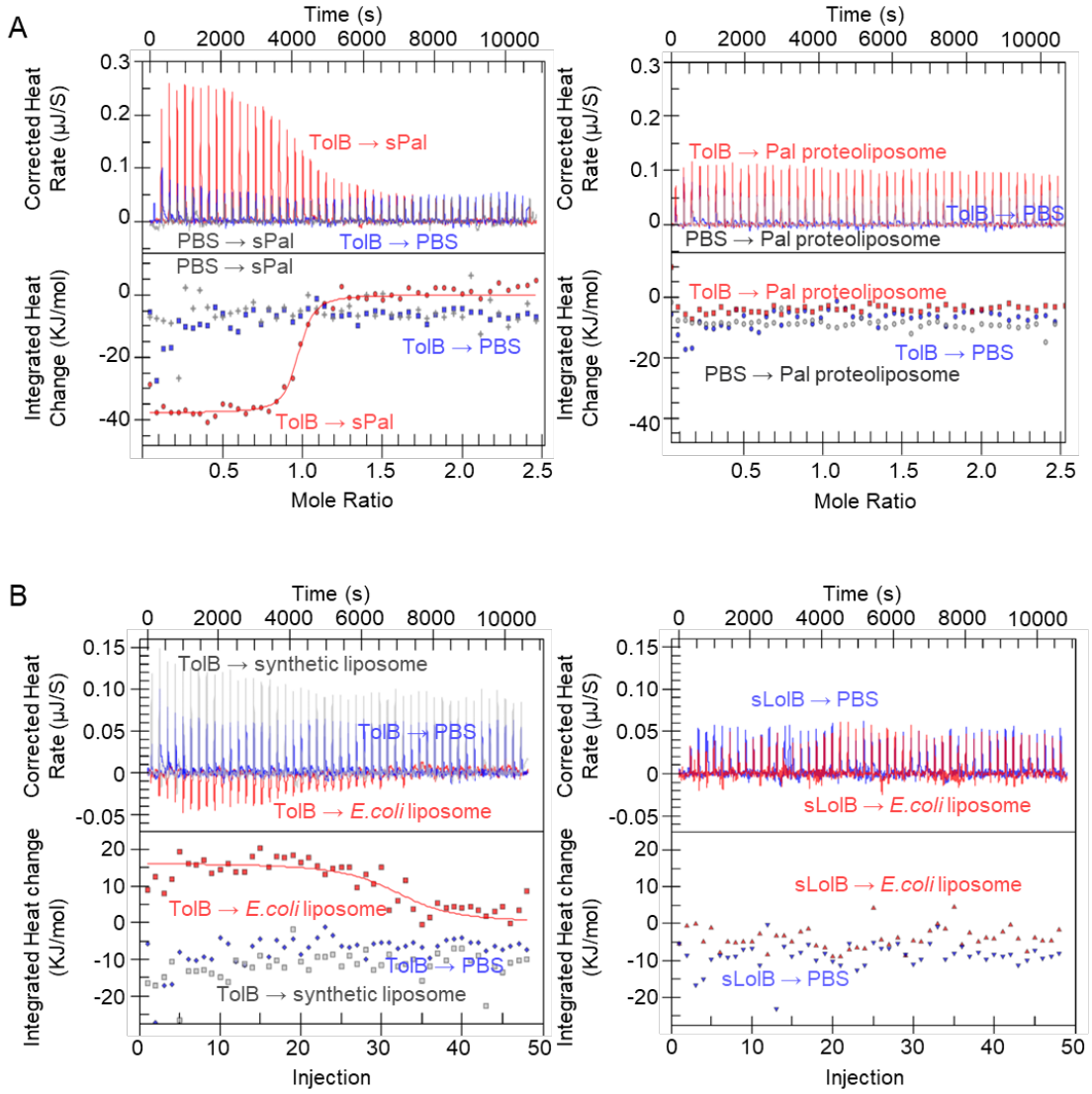


437

438 **Fig 1: TolB interacts with lipid bilayers in vitro.** (A) Representative ITC data for TolB (140
439 µM, 7 nmol) titrated into (*left*) soluble Pal (sPal, 20 µM, 3.32 nmol) or (*right*) Pal
440 proteoliposomes (25 µM, 3.32 nmol surface-exposed) in phosphate-buffered saline (PBS),
441 with indicated control titrations. (B) Representative ITC data for (*left*) TolB or (*right*) LolB (140
442 µM, 7 nmol) titrated into empty liposomes (5 mg lipids) composed of *E. coli* polar lipid extract
443 (PE:PG:CL ~67:23:10) or synthetic lipids (PE:PG 3:1), with indicated control titrations. Each
444 titration was performed at 25 $^{o}$C, and repeated more than 3 times.

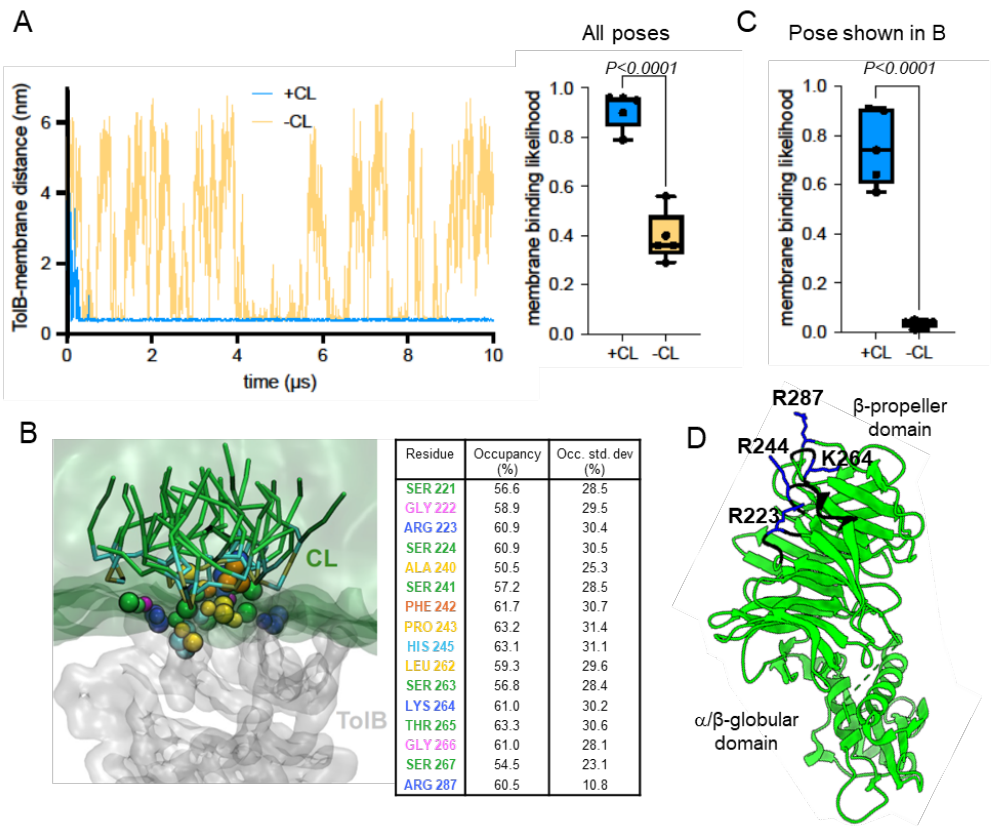


| Residue | Occupancy (%) | Occ. std. dev (%) |
|---|---|---|
| SER 221 | 56.6 | 28.5 |
| GLY 222 | 58.9 | 29.5 |
| ARG 223 | 60.9 | 30.4 |
| SER 224 | 60.9 | 30.5 |
| ALA 240 | 50.5 | 25.3 |
| SER 241 | 57.2 | 28.5 |
| PHE 242 | 61.7 | 30.7 |
| PRO 243 | 63.2 | 31.4 |
| HIS 245 | 63.1 | 31.1 |
| LEU 262 | 59.3 | 29.6 |
| SER 263 | 56.8 | 28.4 |
| LYS 264 | 61.0 | 30.2 |
| THR 265 | 63.3 | 30.6 |
| GLY 266 | 61.0 | 28.1 |
| SER 267 | 54.5 | 23.1 |
| ARG 287 | 60.5 | 10.8 |

**Fig 2: TolB interacts with CL in silico via a putative binding site.** (A) Analysis of TolB-membrane distance over time in a representative 10-μs coarse-grain MD simulation, in the presence or absence of CL. Membrane binding likelihood, averaged over 5 repeat runs, considering all binding poses, is shown on the right. Two-tailed Student's t-test was used to test for statistical significance. (B) The most representative pose of how TolB (*grey*) interacts with CL in coarse-grain simulations, showing residues (colored spheres) in contact with CL molecules (*green/cyan/tan* sticks), and their percentage CL occupancies (in table). (C) Membrane binding likelihood, just considering the binding pose in (B). (D) Contact residues are mapped onto a cartoon representation of TolB structure. Basic or other residues are colored *blue* (with side chain) or *black* (backbone only), respectively.

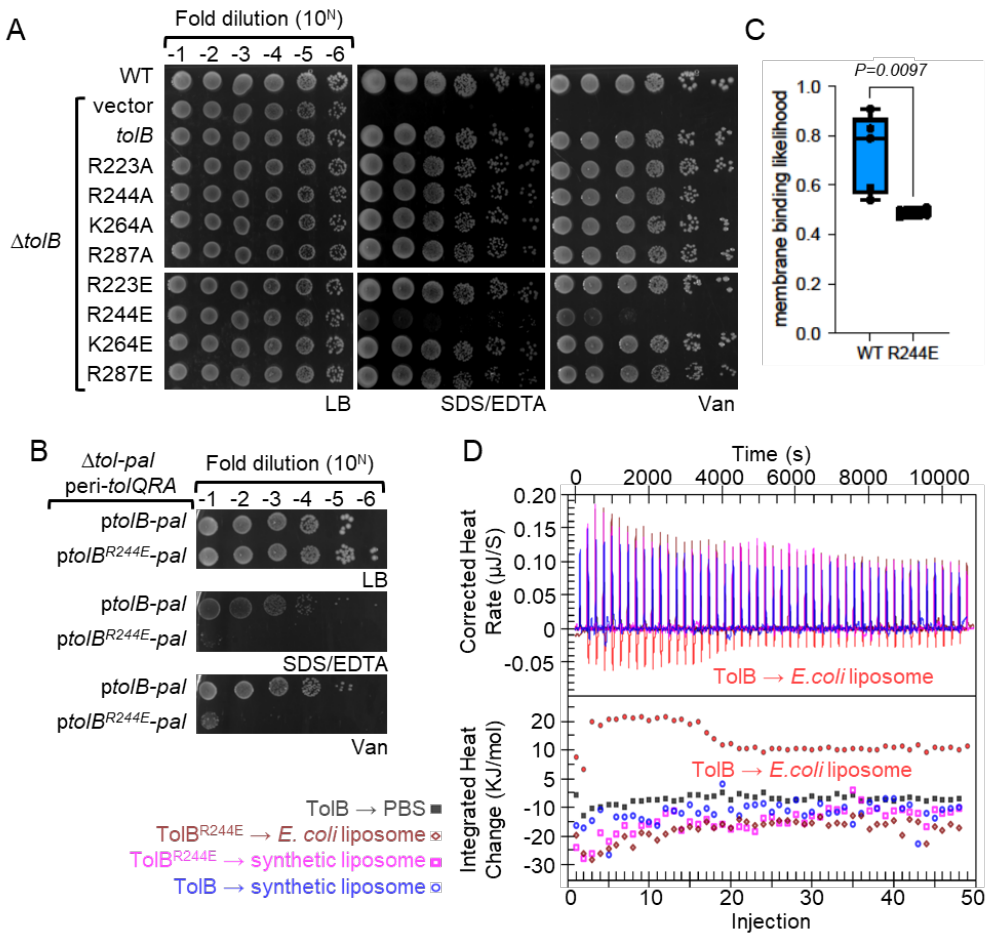


456

457 **Fig 3: Mutation within putative CL-binding site resulted in loss of TolB function.** (A)
458 Efficiency of plating (EOP) of MG1655 wild type (WT), and Δ*tolB* strains, containing either
459 pET22/42 empty vector or the plasmid expressing TolB and its mutants, on LB agar plates
460 supplemented with SDS/EDTA (0.5% SDS/0.5 mM EDTA) or vancomycin (60 μg/mL) at 37°C.
461 (B) EOP of MG1655 Δ*tol-pal* strain expressing a peripheral version of the TolQRA complex
462 that remains randomly distributed along the cell periphery, and is known to restore OM
463 defects,[10] containing either pBAD43-*tolB-pal* or pBAD43-*tolB*$^{R244E}$*-pal*, on LB agar plates
464 supplemented with SDS/EDTA (0.3% SDS/0.3 mM EDTA) or vancomycin (30 μg/mL) at 37
465 °C. Peripheral TolQRA is engineered using a chimeric TonB-TolA that complexes with ExbBD
466 (homolog of TolQR). (C) Membrane binding likelihood, averaged over 5 x 10 μs MD runs, of
467 wild-type TolB and TolB$^{R244E}$ binding to CL-containing membrane. (D) Representative ITC data
468 of TolB and TolB$^{R244E}$ (140 μM, 7 nmol) titrated into *E. coli* or synthetic liposomes (5 mg lipids)
469 at 25 °C, with indicated control titrations.

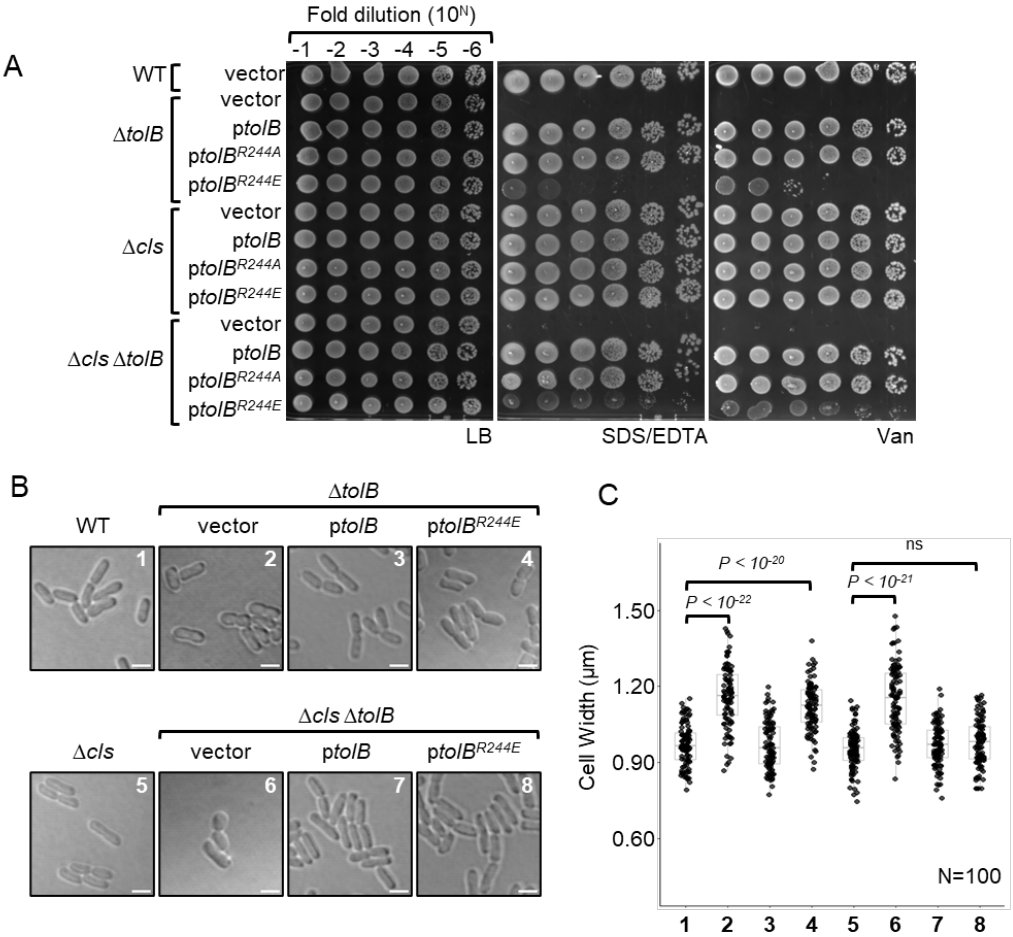


**Fig 4: TolB$^{R244E}$ regains partial function in strains without CL.** (A) EOP of MG1655 wild type (WT), Δ*tolB*, Δ*cls*, and Δ*cls* Δ*tolB* strains, containing either pET22/42 empty vector or the plasmid expressing TolB and its mutants, on LB agar plates supplemented with SDS/EDTA (0.5% SDS/0.5 mM EDTA) or vancomycin (60 µg/mL) at 37 °C. (B) Differential interference contrast (DIC) microscope images of indicated strains from (A) grown in LB at 37 °C. Scale bar represent 2 µm. Cropped images are representative of at least three different uncropped field-of-view. (C) Quantification of the cell width of 100 individual cells of same strains (numbered) shown in (B). Box plot defines the median (center) and the 25$^{th}$ and 75$^{th}$ percentile (lower and upper hinge); the whisker represents the range excluding the outliers (outlier defined by sample with value further than 1.5 interquartile-range from the corresponding hinge). A two-sided Wilcoxon ranked sum test was used to test for statistical significance.

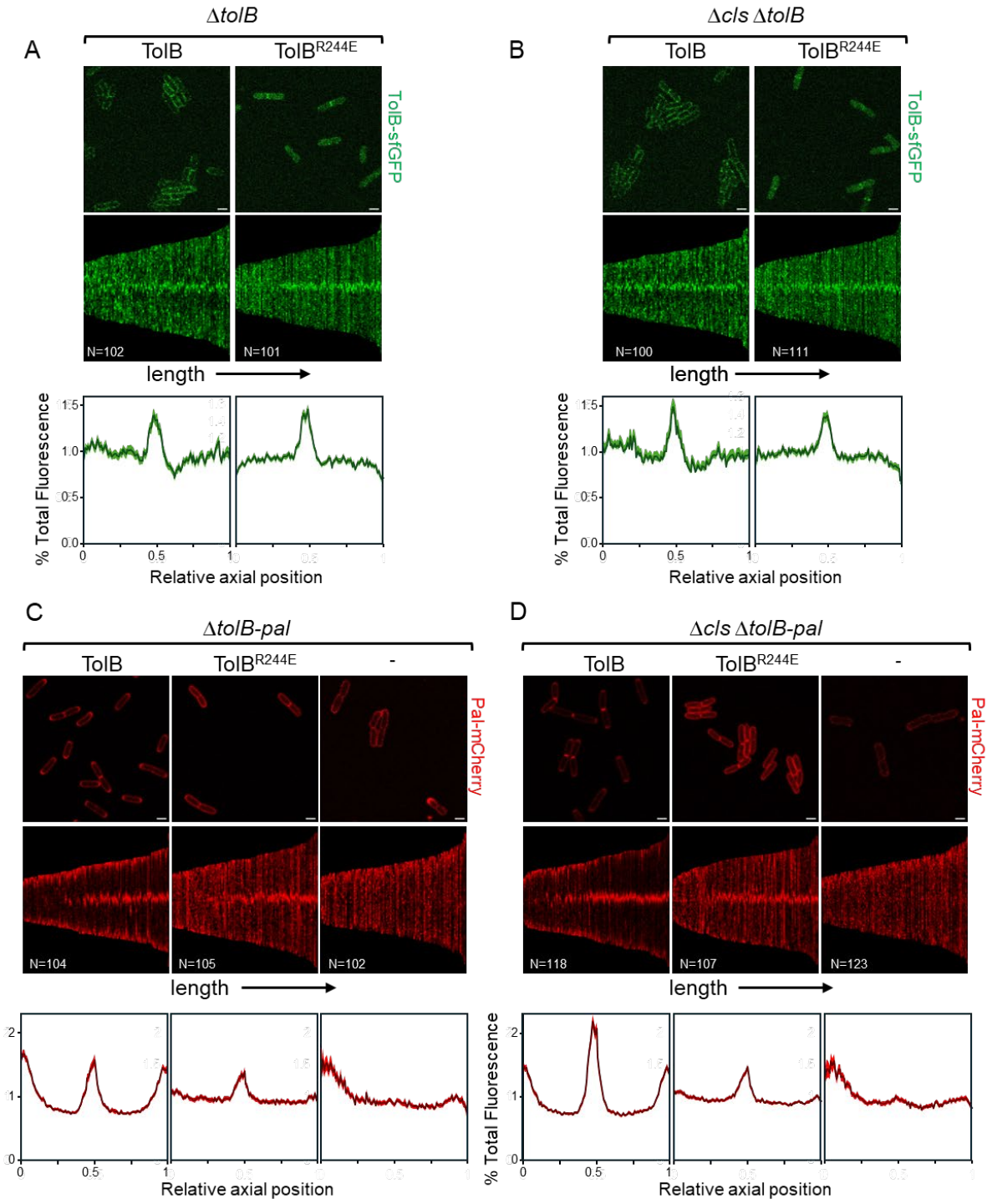


482

483 **Fig 5: TolB and Pal still localize to cell septa in the presence of *tolB*$^{R244E}$ mutation, and/or**
484 **in the absence of CL.** (*top*) Fluorescence microscopy images of (A) MG1655 Δ*tolB::kan* and
485 (B) Δ*cls* Δ*tolB::kan* strains, expressing TolB-sfGFP or TolB$^{R244E}$-sfGFP from pET22/42, and of
486 (C) MG1655 Δ*tolB-pal::kan* and (D) Δ*cls* Δ*tolB-pal::kan* strains, expressing Pal-mCherry,
487 TolB/Pal-mCherry or TolB$^{R244E}$/Pal-mCherry from pBAD43. Scale bar represents 2 µm. (*middle*)
488 Demographic representation of the fluorescence signals in the indicated strains measured
489 along the long axis of individual cells, sorted according to cell length and aligned to mid-cell.

490 (*bottom*) Average percentage distribution of the fluorescence signals along the long axis of all
491 cells measured, where the relative axial position of 0.5 corresponds to mid-cell, and 0 to 1
492 correspond to the poles.